# Brain MR Image Segmentation using Fuzzy Entropy-based Clustering Algorithm

*Thesis submitted in partial fulfillment of the requirements for the degree of*

**Master of Technology**
**in**
**Computer Technology**

*Submitted by*

**Ritama Sharma**
**Regn. No. - 160103 of 2021-2022**
**Exam Roll No. - M6TCT24026**
**Class Roll No. - 002110504032**
**Session - 2021 - 2024**

*Under the supervision of*

**Prof. (Dr.) Jamuna Kanta Sing**

*Department of Computer Science and Engineering*
*Faculty Council of Engineering and Technology*
*Jadavpur University*
*188, Raja S.C. Mallick Rd,*
*Kolkata - 700032, West Bengal, India*

**Department of Computer Science and Engineering**
**Faculty Council of Engineering and Technology**
**Jadavpur University, Kolkata - 700032**

# CERTIFICATE OF RECOMMENDATION

This is to certify that the work embodied in this thesis entitled **"Brain MR Image Segmentation using Fuzzy Entropy based Clustering Algorithm"** has been satisfactorily completed by **Ritama Sharma (Registration Number 160103 of 2021-2022; Class Roll No. 002110504032; Examination Roll No. M6TCT24026)**. It is a bonafide piece of work carried out under my supervision and guidance at Jadavpur University, Kolkata, for partial fulfilment of the requirements for the awarding of the **Master of Technology** in **Computer Technology** degree of the Department of Computer Science and Engineering, Faculty Council of Engineering and Technology, Jadavpur University, during the academic year 2021 - 2024.

---

**Prof. (Dr.) Jamuna Kanta Sing**,
**(Supervisor)**
Department of Computer Science and Engineering,
Jadavpur University,
Kolkata - 700032

Forwarded By:

---

**Prof. (Dr.) Nandini Mukhopadhyay**,
Head of the Department,
Department of Computer Science and Engineering,
Jadavpur University,
Kolkata - 700032

---

**Prof. (Dr.) Dipak Laha**,
DEAN,
Faculty Council of Engineering and Technology,
Jadavpur University,
Kolkata - 700032

**Department of Computer Science and Engineering**
**Faculty Council of Engineering and Technology**
**Jadavpur University, Kolkata - 700032**

# CERTIFICATE OF APPROVAL

This is to certify that the thesis entitled **"Brain MR Image Segmentation using Fuzzy Entropy based Clustering Algorithm"** is a bonafide record of work carried out by **Ritama Sharma (Registration Number 160103 of 2021-2022; Class Roll No. 002110504032; Examination Roll No. M6TCT24026)** in partial fulfilment of the requirements for the award of the degree of **Master of Technology** in **Computer Technology** in the **Department of Computer Science and Engineering, Jadavpur University**, during the period of July 2023 to May 2024. It is understood that by this approval, the undersigned do not necessarily endorse or approve any statement made, opinion expressed or conclusion drawn therein, but approve the thesis only for the purpose of which it has been submitted.

_____
Signature of Examiner 1
Date:

_____
Signature of Examiner 2
Date:

**Department of Computer Science and Engineering**
**Faculty Council of Engineering and Technology**
**Jadavpur University, Kolkata - 700032**

# DECLARATION OF ORIGINALITY AND COMPLIANCE OF ACADEMIC ETHICS

I hereby declare that the thesis entitled **"Brain MR Image Segmentation using Fuzzy Entropy based Clustering Algorithm"** contains literature survey and original research work by the undersigned candidate, as a part of her degree of **Master of Technology** in **Computer Technology** in the **Department of Computer Science and Engineering, Jadavpur University**. All the information have been obtained and presented in accordance with academic rules and ethical conduct.

I also declare that, as required by these rules and conduct, I have fully cited and referenced all materials and results that are not original to this work.

**Name:** Ritama Sharma

**Examination Roll No.:** M6TCT24026

**Registration No.:** 160103 of 2021-2022

**Thesis Title:** Brain MR Image Segmentation using Fuzzy Entropy based Clustering Algorithm

**Signature of the Candidate:**

# *Acknowledgements*

I convey my honest and sincere thanks to my respected teacher and my guide ***Prof. (Dr.) Jamuna Kanta Sing***, Professor of Department of Computer Science & Engineering, Jadavpur University, for his exclusive guidance and undivided support in completing and presenting this thesis successfully. I am indebted to him for the constant encouragement and continuous inspiration that he has given me. The above words are only a token of my deep respect towards him for all that he has done to take my thesis to its present shape.

I would also like to thank ***Mrs. Madhumita Ray*** for her valuable suggestions and key insights that she has provided while working on this thesis.

Finally, I express my sense of gratitude and thanks to my family members, especially my mother for her unconditional love and support. Last but not the least I am grateful to all my friends for staying beside me and being an endless source of optimism and positive thoughts.

---

**Ritama Sharma**

Examination Roll No.: M6TCT24026

Registration No.: 160103 of 2021-2022

Department of Computer Science and Engineering,

Jadavpur University

# Contents

**Table of Contents** i

**List of Figures** i

**List of Tables** iii

**Abstract** iv

**1 Introduction** 1
- 1.1 Image Segmentation . . . 1
- 1.2 Brain MR Image Segmentation . . . 2

**2 Literature Survey** 4
- 2.1 Image Segmentation Methods . . . 4

**3 Fuzzy Entropy-based Clustering Algorithm** 8
- 3.1 Concept of Entropy . . . 8
  - 3.1.1 Shannon Entropy . . . 9
  - 3.1.2 Renyi Entropy . . . 9
  - 3.1.3 Kapur Entropy . . . 9
  - 3.1.4 Vajda Entropy . . . 10
- 3.2 Fuzzy Entropy-based Clustering Algorithm . . . 10
- 3.3 Quantitative Evaluation Metrics . . . 13
  - 3.3.1 Cluster Validity Functions . . . 13
  - 3.3.2 Segmentation Accuracy($SA$) . . . 14
  - 3.3.3 Tissue Segmentation Accuracy($TSA$) . . . 15

**4 Experimental Results** 16
- 4.1 Result obtained on BrainWeb Dataset . . . 16
  - 4.1.1 T1-Weighted image volume . . . 17

**5 Conclusion** 31

**Bibliography** 32

# List of Figures

1.1 Brain MR Image . . . . . 3

4.1 Original to Cluster 4 shows the qualitative segmentation results of the Original image, segmented Background image, segmented CSF image, segmented GM image, segmented WM image (from left to right) by the proposed method, on slice 82 of T1-Weighted MR image volume having 9% noise, 40% inhomogeneity. . . . . 17
4.2 Original to Cluster 4 shows the qualitative segmentation results of the Original image, segmented Background image, segmented CSF image, segmented GM image, segmented WM image (from left to right) by the proposed method, on slice 92 of T1-Weighted MR image volume having 9% noise, 40% inhomogeneity. . . . . 18
4.3 Similarity Index ($\rho$) of proposed and other methods . . . . . 20
4.4 Partition Coefficient ($V_{pc}$) of proposed and other methods . . . . . 21
4.5 Partition Entropy ($V_{pe}$) of proposed and other methods . . . . . 22
4.6 Segmentation Accuracy (CSF) of proposed and other methods . . . 24
4.7 Segmentation Accuracy (GM) of proposed and other methods . . . 25
4.8 Segmentation Accuracy (WM) of proposed and other methods . . . 26
4.9 Tissue Segmentation Accuracy (CSF) of proposed and other methods 28
4.10 Tissue Segmentation Accuracy (GM) of proposed and other methods 29
4.11 Tissue Segmentation Accuracy (WM) of proposed and other methods 30

# List of Tables

4.1 Comparative study of average value of Cluster Validity Function (SI ($\rho$), $V_{pc}$, $V_{pe}$) on 51 T1-weighted MRI brain images each in an image volume using different algorithms. . . . . 19
4.2 Comparative study of average value of Segmentation Accuracy (SA) on 51 T1-weighted MRI brain images each in an image volume using different algorithms. . . . . 23
4.3 Comparative study of average value of Tissue Segmentation Accuracy (TSA) on 51 T1-weighted MRI brain images each in an image volume using different algorithms. . . . . 27

# *Abstract*

In this thesis work, we proposed an image segmentation method that is based on fuzzy c-means algorithm. It has been modified by Shannon entropy by which we can segment a noisy 2D brain MR image which also contains high Intensity Inhomogeneity (IIH). We fail to achieve comparable segmentation accuracy using standard Fuzzy Clustering Algorithm (FCM). As the segmentation is not so perfect, it becomes hard to find the abnormality or the diseases in the tissue areas in brain. To reduce this problem, we considered many algorithms that are based on standard FCM algorithm. Among them the entropy based clustering algorithms reduces the uncertainty of a pixel being in a cluster. Those algorithms perform well in some scenarios but appears to fail in majority of cases. In this thesis, we tried to improve the performance of a particular entropy based clustering algorithm. A very detailed comparative analysis has been made with different cases also including a contrast with previous algorithms. The new segmentation method was applied to BrainWeb brain MR database at varying noise and inhomogeneity. It gives us a better segmentation result when evaluated in terms of Dice Similarity Coefficient, Partition Coefficient, Partition Entropy, Segmentation Accuracy, Tissue Segmentation Accuracy.

CHAPTER 1

# Introduction

## 1.1 Image Segmentation

Image segmentation is a fundamental process in computer vision [1] and image processing that involves dividing a digital image into distinct regions or segments. These segments are typically based on certain criteria such as pixel intensity, color, texture, or other visual features. The goal of image segmentation is to simplify the representation of an image, making it easier [2] to analyze and extract meaningful information. It is commonly used in various applications such as object detection, medical image analysis [3], satellite imaging, robotics, and more.

In image classification, it enables object recognition crucial for applications like autonomous vehicles and surveillance, aids in content understanding and organization for tasks such as image retrieval and data analysis, supports decision-making processes like medical diagnosis, and contributes to automation and efficiency in domains like agriculture and retail [4]. Moreover, image classification serves as foundational training data for machine learning and AI models, ensuring continual improvement and reliability in various technological applications.

Image segmentation offers numerous advantages across diverse applications. It enables accurate object detection and recognition by delineating objects within an image, facilitating tasks like tracking and diagnosis in medical imaging. Segmented images provide a clearer and organized view, aiding in enhanced analysis [5], efficient compression, and semantic understanding of visual content. This segmentation also improves image editing precision, serves as valuable training data for machine learning algorithms, and enhances visualization for effective communication and presentation of information, contributing significantly to advancements

in computer vision, medical imaging, remote sensing, and multimedia processing.

Image segmentation encompasses various techniques, it can be divided into five parts like: thresholding, clustering, edge detection, region growing and deep learning-based segmentation [4]; each segmentation technique has its strengths and limitations, and the choice depends on the specific requirements of the application, such as the nature of the images, the complexity of objects to be segmented, and the desired level of accuracy.

## 1.2 Brain MR Image Segmentation

Brain MR (Magnetic Resonance) image [6], [7] segmentation is a critical task in medical image analysis with various applications in diagnosis, treatment planning, and research. Any kind of abnormalities could be identified by tracking of changes in volume, shape and regional distribution of brain tissue. It involves dividing a brain MRI [8], [9] scan into different regions or structures, such as Cerebrospinal fluid (CSF), Grey matter (GM), White matter (WM) [10] to extract meaningful information for medical professionals. The Internet Brain Segmentation Respository (IBSR) provided by the Center for Morphometric Analysis (CMA) at Massachusetts General Hospital and BrainWeb, which has been collected at McConnell Brain Imaging Centre of the Montreal Neurological Institute, McGill University are two popular datasets generally used in this domain of research [11].

Brain MR image segmentation offers crucial advantages in medical imaging, aiding in accurate diagnosis of neurological disorders like tumors, multiple sclerosis, and Alzheimer's disease by providing detailed tissue information. It facilitates treatment planning, such as surgical interventions and radiation therapy, by visualizing tumor locations and brain structures. Additionally, segmentation supports research and quantitative analysis, advancing medical knowledge and enabling the integration of MRI data with other imaging modalities for enhanced diagnostic accuracy and patient care.

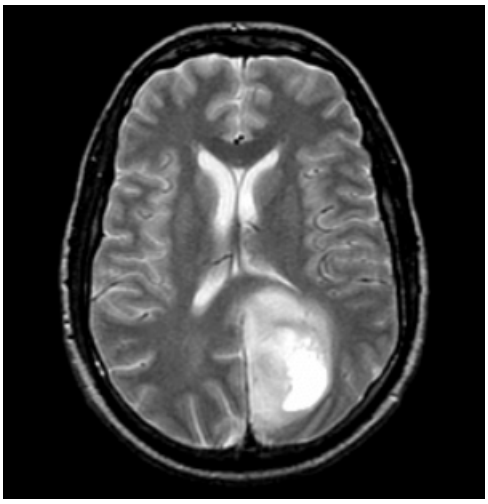


Figure 1.1: Brain MR Image

In 2D space we can represent an image like $I(i, j)$ where $i = 0, 1, 2, ..., M - 1$, $j = 0, 1, 2, ..., N - 1$ denotes spatial coordinates. The function $I(i, j)$ gives the intensity value of a particular pixel and that intensity value lies in between $[0-255]$ i.e the grey value of the brain MR (Magnetic Resonance) image [12]. Every image consists of a finite set of image elements, called pixels in 2D space. Each image is uniquely defined by its intensity value and the coordinates i.e $I(i, j)$ for pixels where, $i$ is the image row number and $j$ is the image column number [12].

CHAPTER 2

# Literature Survey

## 2.1 Image Segmentation Methods

The fuzzy entropy clustering algorithm is a method used for data clustering, particularly in scenarios where traditional clustering methods may not be suitable due to data uncertainty or fuzziness. It combines the concepts of fuzzy logic and entropy to partition data into clusters based on the degree of uncertainty or randomness associated with each data point's membership to a cluster.

Here are some key aspects of the fuzzy entropy clustering algorithm: (a) Fuzzy Logic, (b) Entropy, (c) Objective Function, (d) Iterative Optimization.

Advantages of the fuzzy entropy clustering algorithm include its ability to handle data uncertainty, accommodate overlapping clusters, and provide interpretable cluster assignments based on fuzzy memberships and entropy measures. These advantages make it particularly suitable for clustering tasks in complex and uncertain datasets, such as in image segmentation, pattern recognition, and data mining applications.

There are a number of algorithms for segmentation of medical images such as, MRI images have been presented in the past. Among them, intensity thresholding, region-based segmentation, edge-based segmentation and classification-based segmentation are the most frequently used techniques [13], [14] for segmenting MR images.

In intensity thresholding, the threshold level is automatically determined from the grey-level histogram of the image[15]. The distribution of intensities in medical images, especially in MRI images is usually very complex as stated above, and

therefore, thresholding methods fail due to lack of determining optimal threshold. In addition, intensity thresholding methods have disadvantage of spatial uncertainty as the pixel location information is ignored. So, we need to determine the optimal threshold.

The edge-based approaches [16] first generate interrupted (scattered) contour lines around an object of interest using some edge detection algorithms. Next, these contour lines are joined based on some similarity criteria to detect the object of region of interest (ROI). However,these methods usually require computationally expensive post-processing to obtain hole free representation of the objects. The region growing methods extend the thresholding by integrating it with connectivity by means of an intensity similarity measure. These methods start with a seed point (pixel) for each region and during the region growing, pixels in the neighbourhood are added to the regions based on homogeneity criteria, resulting connected regions. However, they are sensitive to noise and thus less suitable for medical image segmentation.

Apart from fuzzy logic based statistical methods, Some other methods based on Convolutional Neural Networks (CNN) are proposed [17], [18]. They proposed a method for Brain tumor segmentation in MR images using deep convolutional neural networks, exploiting small convolutional kernals. The architecture stacks more convolutional layers having same receptive fields as of bigger kernals. It combines multiple patch and kernal sizes to learn multi-scale features, which estimate both the intensity and spatial characteristics. However, the main disadvantage of convolutional neural network is that it requires high computational time during its training phase. The methods so far discussed do not use entropy while segmenting brain MR images. However, some authors proposed that use entropy in the objective function for classification of noisy data [19]–[23].

FCM clustering algorithm is more efficient in Classification-based segmentation method, than the other hard clustering methods,like k-means algorithm etc. FCM [15] algorithm allows pixels to have relation with multiple clusters with varying degree of membership, so it is more reasonable in real applications. FCM is no doubt a very popular unsupervised clustering method, but it has some limitations due to consideration of the image spatial information. It has another serious disadvantages of local optimal solution due to poor initialization. Many modified fuzzy clustering approaches have been reported in the past for making the FCM algorithm more robust to noise and outliers for image segmentation.

Pedryca [16] introduced a conditional FCM based clusterting method guided

by an auxiliary or conditional variable. The method reveals a structure within a group of patterns by considering their vicinity in a feature space along with the similarity of the values assumed by a certain conditional variable. The FCM algorithm through the incorporation of the spatial information. They introduced the spatial information into the computation of similarity measure. The similarity measure is modified to drag a pixel closure to the cluster center if it is in homogenous region. The disadvantages of this algorithm are its sensitivity to the non-descriptive initial clusters and its massive computational loads.

Selvathi [24] presented a modified version of the spatial FCM algorithm to classify the pixels. For MRI brain image segmentation by incorporating intensity inhomogeneity and spatial information by using probabilistic FCM algorithm. The method works in two steps. First it estimates the intensity inhomogeneity or bias field in the MR medical images. The intensity inhomogeneity or intensity non-uniformity usually refers to the slow, non-anatomic intensity variations of the same tissue over the image domain and causes due to imperfection of the image acquisition devices, eddy current, poor magnetic field and patient movement etc. Then the inhomogeneity is corrected by using fusion of suitable Gaussian surfaces which are obtained from calculating the gradient map of different homogenous regions. After this process the corrected image is segmented using a modified probabilistic FCM clustering algorithm that takes into consideration the spatial features of pixels of the image.

Wang [25] introduces a modified fuzzy c-means clustering algorithm by utilizing local contextual information and high correlation inherent between the inter-pixel. In this model at first a local similarity measure model is established and then based on local spatial similarity measure model, cluster center and membership values are initialized. Then secondly, based on the high correlation inherent between the inter-pixel, the fuzzy membership function is modified accordingly.

Noordam [26] describes a technique in his paper that is how to overcome the sensitivity of fuzzy c-means clustering for the different cluster sizes in multivariate images. This paper proposed a modified version of standard FCM, called conditional FCM which is used to balance the unequal sized cluster. The ratio between the cluster sizes are determined and a condition value is calculated during the clustering process. The influence of objects from larger clusters to smaller clusters is balanced by the condition value. Considering the INU (Intensity Non-uniformity) a spatial information by using fuzzy c-means clustering algorithm, with the help of fusion of Gaussian surfaces, one can correct the INU of MR image of brain.

The individual Gaussian surface is evaluated independently over the different homogeneous regions under consideration of its center as the center of the respective homogeneous region.

Qiu [27] suggested a novel algorithm for fuzzy segmentation by introducing two fuzzifiers and a spatial constraint in the membership function. Another improvement of the FCM clustering algorithm using PSO, Mahalanobis distance and post segmentation correction. The first step introduced PSO initialization to overcome the problem of local minima in the solution, the second step was concerned with the integration of the spatial gray level information and the Mahalanobis distance and the final step refined the segmentation results by reallocating the potentially misclassified pixels. A class of robust non-Euclidean distance measure for the objective function to enhance the robustness of the original FCM clustering algorithm and to reduce noise and outliers. A fast-spatial constrained fast kernel based fuzzy c-means clustering (FKFCM) algorithm for MR brain image segmentation. The FKFCM algorithm first transforms the pixel intensities into a higher dimensional space using a kernel trick and then performs classification on the transformed data.

CHAPTER 3

# Fuzzy Entropy-based Clustering Algorithm

## 3.1 Concept of Entropy

In our approach we tried to incorporate Shannon entropy with conventional FCM algorithm that can effectively segment brain MR images with the presence of noise and high intensity inhomogeneity (IIH). Fuzzy logic is involved to find the better membership value of a pixel for a particular cluster and entropy is involved because of the dissimilarity between the pixels in the edge region are high.

Entropy uses in various fields like physics, information theory, mathematics and other branches of science and engineering [28]. It was first introduced in thermodynamics developing an information theoretical concept which is closely connected to the internal energy of the system. Entropy can be defined as uncertainty or the amount of disorder present in an information that is being processed in machine learning. The other way we can explain that entropy is the standard approach that helps to measure the unpredictability and the impurity presents in the system. Actually, it is the measure of the degree of uncertainty that can be used to characterize the texture of the image we used.

Entropy is formulated as below [29], [30]:

$$-\sum p_i \times \log p_i \tag{3.1}$$

where $p_i$ is the probability of given symbol.

There are various types of entropies for significant applications. Some of them are discussed in the following section:

### 3.1.1 Shannon Entropy

Shannon entropy gives us an absolute limit on the best possible lossless compression of signal under constraint. Suppose, X is a random variable, then Shannon entropy can be defined as

$$H(X) = -\sum p(x_i) \log p(x_i) \tag{3.2}$$

In 2D random space, $p(x_i)$ is probability density function [31].

### 3.1.2 Renyi Entropy

It is generalized version of Shannon entropy. It is used for quantum information to measure the entanglement. It is defined as the entropy of order on $\alpha$, where $\alpha \geq 0$ and $\alpha \neq 1$, is defined as:

$$H_r(X) = \frac{1}{(1-\alpha)} \log \sum p_i^{\alpha} \tag{3.3}$$

For noisy cell image segmentation Sadek [32] proposed an efficient and faster entropy based method, based on generalized $\alpha$ - entropy by calculating the maximum structural information of image and according to desired segmentation, have to locate the optimal threshold. High rapidity and it's tolerance is the advantage of their proposed algorithm in the presence of noise in the image.

### 3.1.3 Kapur Entropy

This entropy is denoted by $H_k(X)$ of order of $\alpha$ and type $\beta$, is written as [33] :

$$H_k(X) = \left( \frac{\sum p_i^{\alpha+\beta-1}}{\sum p_i^{\beta}} \right) (2^{1-\alpha} - 1)^{-1} \tag{3.4}$$

### 3.1.4 Vajda Entropy

This entropy is a special case of Kapur entropy where $\beta = 1$ is taken and the uncertainty is calculated. Vajda entropy takes less time as its calculation is faster as compared to the Kapur's entropy. So, it is preferable than Kapur's entropy. It is defined as follows [29], [34] :

$$H_v(X) = \left(\frac{\sum p_i^{\alpha}}{\sum p_i} - 1\right)(2^{1-\alpha} - 1)^{-1} \tag{3.5}$$

## 3.2 Fuzzy Entropy-based Clustering Algorithm

Here, we incorporate Shannon entropy in our proposed method to improve the validity of the fuzzy clustering algorithm (FCM). As we know that brain MR images are sensitive to noise [14] and intensity inhomogeneity, it is very difficult to achieve effective results. So, to detect diseased regions in MR image, it is necessary to segment the image into different tissue regions (CSF, GM, WM) accurately. Entropy is proportional to uncertainty, So our aim is to minimize the entropy to obtain better segmented image.

This section is allows to partition the image pixels by calculating the cluster center $v_i$ and the membership matrix $\mu_{ik}$ through minimizing the following Objective function, with respect to the cluster centres and membership degrees in an iterative manner.

$$J = \sum_{i=1}^{C}\sum_{k=1}^{N}\mu_{ik}^{m}\left(1 - e^{-\frac{||x_k - v_i||^2}{2\sigma_k^2}}\right) + \sum_{k=1}^{N}U(x_k) \tag{3.6}$$

Subject to the constraint,

$$\sum_{i=1}^{C}\mu_{ik} = 1 \tag{3.7}$$

Where,

$$U(x_k) = -\sum_{i=1}^{C} P_{ik}\ln(P_{ik}) \tag{3.8}$$

$$P_{ik} = \frac{\sum_{x_j \in N_k}\mu_{ij}}{||N_k||} \tag{3.9}$$

where, $P_{ik}$ is the probability of the pixel intensity $x_k$ to belong to the $i$th class. The value of $p_{ik}$ is ranged in $[0, 1]$. Check if $\sum_{i=1}^{C} P_{ik} = 1$ or not.

Where, $m$ is the fuzziness coefficient $(> 1)$ , $\mu_{ik}$ is the degree of membership of $x_k$ in the cluster $i$, $C$ is the total number of clusters. $U(x_k)$ is the class uncertainty ( the object boundaries of the acquired images are blurred due to the presence of noise and intensity inhomogeneity, in this regard the pixels at the boundary regions are having high value of class uncertainty or entropy) associated with the given pixel intensity $x_i$. $\sigma_k$ denote the standard deviation of the intensity values for the $i$th class.

Consequently, we have incorporated the interaction among adjacent pixels in the fuzzy membership function in such a way that if the neighbouring pixels share similar characteristics, the centre pixel should have higher probability of grouping to the same cluster as of the neighbouring pixels. We have also introduced conditioning aspect into the clustering mechanism. The algorithm takes into consideration the conditioning variable associated with each pixel, which describes the level of involvement for construction of membership functions and different clusters. This is realized by introducing a weighted membership function.

Minimizing the objective function (3.6) with respect to the constraint $\sum_{i=1}^{C}\mu_{ik} = 1$,

We obtain

$$\frac{\partial}{\partial \mu_{ik}}(J) = 0 \tag{3.10}$$

$$\frac{\partial}{\partial v_i}(J) = 0 \tag{3.11}$$

Differentiating the equation (3.6) partially with respect to $\mu_{ik}$, We get the following equation:

$$m\mu_{ik}^{m-1}\left(1-e^{-\frac{||x_k-v_i||^2}{2\sigma_k^2}}\right)-\sum_{i=1}^{C}\sum_{k=1}^{N}P_{ik}\ln(P_{ik})=0 \tag{3.12}$$

$$m\mu_{ik}^{m-1}\left(1-e^{-\frac{||x_k-v_i||^2}{2\sigma_k^2}}\right)=1 \tag{3.13}$$

$$\mu_{ik}^{m-1}=\frac{1}{m\left(1-e^{-\frac{||x_k-v_i||^2}{2\sigma_k^2}}\right)} \tag{3.14}$$

$$\mu_{ik}=\left(\frac{1}{m\left(1-e^{-\frac{||x_k-v_i||^2}{2\sigma_k^2}}\right)}\right)^{\frac{1}{m-1}} \tag{3.15}$$

Using equation $\sum_{j=1}^{C}\mu_{jk}=1$ we get,

$$\sum_{j=1}^{C}\left(\frac{1}{m\left(1-e^{-\frac{||x_k-v_j||^2}{2\sigma_k^2}}\right)}\right)^{\frac{1}{m-1}}=1 \tag{3.16}$$

From equation 3.15 and 3.16 we get,

$$\mu_{ik}=\frac{1}{\sum_{j=1}^{C}\left(\frac{1-e^{-\frac{||x_k-v_i||^2}{2\sigma_k^2}}}{1-e^{-\frac{||x_k-v_j||^2}{2\sigma_j^2}}}\right)^{\frac{1}{m-1}}} \tag{3.17}$$

Similarly, using equation 3.8 in deriving equation 3.6 partially with respect to $v_i$, we get the following equation,

$$\sum_{k=1}^{N}(-1)\mu_{ik}^{m}2(x_k-v_i)[p_{ik}(1+\ln p_{ik})]=0 \tag{3.18}$$

$$\sum_{k=1}^{N}\mu_{ik}^{m}x_k+\sum_{k=1}^{N}p_{ik}(1+\ln p_{ik})=\sum_{k=1}^{N}\mu_{ik}^{m}v_i+\sum_{k=1}^{N}p_{ik}(1+\ln p_{ik}) \tag{3.19}$$

$$v_i=\frac{\sum_{k=1}^{N}[\mu_{ik}^{m}+p_{ik}(1+\ln p_{ik})]x_k}{\sum_{k=1}^{N}[\mu_{ik}^{m}+p_{ik}(1+\ln p_{ik})]} \tag{3.20}$$

Based on the above derivation we have carried out extensive evaluation and analysis on BrainWeb Dataset. In all of the tests that we have executed there are multiple Quantitative evaluation matrix that have been used and they are defined in Succession.

## 3.3 Quantitative Evaluation Metrics

For comparative study, quantitative evaluation is very important. Here, We represented three types of quantitative evaluation based on :

1. Cluster validity functions
2. Segmentation accuracy
3. Tissue segmentation accuracy

The cluster validity functions are represented in terms of
(a) Dice Similarity Coefficient
(b) Partition Coefficient
(c) Partition Entropy

To reduce the influences of the selected images, the results are:

### 3.3.1 Cluster Validity Functions

(a) Dice Similarity Coefficient (DSC) :

Dice Similarity Coefficient (DSC) or Dice Coefficient is a very important performance index as it measures the spatial overlap between the segmentation result and ground truth. It is also known as the similarity index ($\rho$). Let, for an image $C$ clusters, if $A_i$ and $B_i$ represent the set of pixels belonging to a cluster $i$ in the segmented image and in the Ground truth image respectively. Then, the Dice Similarity Coefficient or Dice Coefficient is defined as follows [10], [27] :

$$DSC = \frac{1}{C}\sum_{i=1}^{C}\frac{2|A_i \cap B_i|}{|A_i| + |B_i|} \tag{3.21}$$

The value of Dice Coefficient is ranged in $[0, 1]$ and the optimal clustering result is achieved when $\rho = 1$, with higher value being "better". It is a very efficient validity measurement as it compares the segmentation results with the Ground truth. Noise and inhomogeneity free image is considered here as the Ground truth image.

(b) Partition Coefficient ($V_{pc}$) :

Partition coefficient ($V_{pc}$) is one of the most essential factors of fuzzy partition. This index specifies the confidence factor of a method for a classification task. It provides the best performance with less fuzziness when the value of $V_{pc}$ takes its optimal value as 1, with higher values being "better". It can be formulated as follows [27], [35], [36] :

$$V_{pc} = \frac{\sum_{K=1}^{C} \sum_{i=1}^{N} \mu_{ik}^2}{N} \tag{3.22}$$

(c) Partition Entropy ($V_{pe}$) :

Partition Entropy ($V_{pe}$) is another important index under the cluster validity functions. It measures the uncertainty while classifying the pixels into correct clusters and negating into other clusters. In an ideal case, the value of $V_{pc}$ is 0. It is defined by the following equation [27], [35], [37] :

$$V_{pe} = \frac{-\sum_{K=1}^{C} \sum_{i=1}^{N} \mu_{ik} \log(\mu_{ik})}{N} \tag{3.23}$$

### 3.3.2 Segmentation Accuracy($SA$)

The Segmentation Accuracy ($SA$) of a clustering algorithm can be defined as the ratio of the number of correctly classified pixels and the actual number of corresponding pixels in the Ground truth. It can be represented as follows [35], [38] :

$$SA = \frac{Card(A_k \cap G_k)}{Card(G_k)} \tag{3.24}$$

The algorithm is said to be better if the value of $SA$ is closer to "1" and in the ideal case, its value is equal to 1.0. In the above expression, $A_k$ depicts the total number of pixels associated with cluster $k$ in the segmented image. Whereas, $G_k$ denotes the total number of pixels associated with the $k$th cluster in the Ground truth.

### 3.3.3 Tissue Segmentation Accuracy($TSA$)

The performance of the proposed method is assessed by evaluating the tissue segmentation accuracy. We have compared tissue segmentation accuracy ($TSA$) with that of other fuzzy based methods to demonstrate the supremacy of our method. The $TSA$ can be expressed as follows [10] :

$$TSA = \frac{N_{ck}}{N_{gk} + N_{dk}} \tag{3.25}$$

In the above definition, $N_{ck}$ is the correctly classified pixels to $k$ tissue which is inside the Ground truth mask. $N_{gk}$ denotes the total number of pixels of $k$ tissue which includes the inside and outside of Ground truth mask. $N_{dk}$ represents the number of pixels of tissue $k$ in the discrete anatomical model. For an ideal result, TSA will be 1, with higher values being "better".

CHAPTER 4

# Experimental Results

The proposed entropy based fuzzy c-means algorithm is validated on the BrainWeb Dataset [39] specifically on the Simulated T1-Weighted images and Simulated T2-Weighted images in both quantitative and qualitative manner. The brain image volumes are segmented in four basic clusters ($C = 4$), they are - (a) Background (BG), (b) Cerebrospinal fluid (CSF), (c) Gray Matter (GM), (d)White Matter (WM).

## 4.1 Result obtained on BrainWeb Dataset

We have downloaded the simulated T1-Weighted and T2-Weighted MR images of human brain with varying noise and inhomogeneity from the BrainWeb provided by McConnel Brain Imaging Center of the Montreal Neurological Institutre, McGill University [40]. In this context, we have illustrated the results for four different volumes of both simulated T1-Weighted and T2-Weighted data volumes with 7% and 9% of noise each having 20% and 40% inhomogeneity has been carried out on volumes of 51 (image slice $50 - 100$) out of total volume of 181. All of the image volumes the resolution is $181 \times 217 \times 181$ and the size is $1mm \times 1mm \times 1mm$. The image volume contains images from the following combination respectively:

(a) 7% noise, 20% inhomogeneity
(b) 7% noise, 40% inhomogeneity
(c) 9% noise, 20% inhomogeneity
(d) 9% noise, 40% inhomogeneity

The performance of the proposed method is examined by a comparative study with k-means, FCM, FGFCM, sFCM, ASIFC methods [10].

### 4.1.1 T1-Weighted image volume

First, we shows the qualitative segmentation results of the Original image, segmented Background image, segmented CSF image, segmented GM image, segmented WM image (from left to right) respectively in figure 1.1 . By the proposed method, on slice 82 of T1-Weighted MR image volume having 9% noise, 40% inhomogeneity.

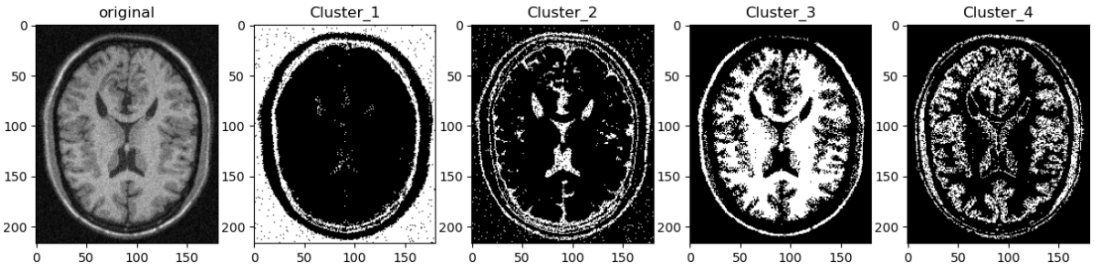



Figure 4.1: Original to Cluster 4 shows the qualitative segmentation results of the Original image, segmented Background image, segmented CSF image, segmented GM image, segmented WM image (from left to right) by the proposed method, on slice 82 of T1-Weighted MR image volume having 9% noise, 40% inhomogeneity.

We shows the qualitative segmentation results of the Original image, segmented Background image, segmented CSF image, segmented GM image, segmented WM image (from left to right) respectively in figure 4.1 . By the proposed method, on slice 92 of T1-Weighted MR image volume having 9% noise, 40% inhomogeneity.

To reduce the influence of the selected images, results are provided as the average values of 51 images (Slice 50 - Slice 100) from each image volume of simulated brain MR images for the Cluster Validity Functions, Segmentation Accuracy, Tissue Segmentation Accuracy.

In the table 4.1 Shows the average values of different Cluster Validity Function, i.e. Similarity Index ($\rho$), Partition Coefficient ($V_{pc}$) and Partition Entropy ($V_{pe}$) of six different algorithms: The k-means, FCM, FGFCM, sFCM, ASIFC and the proposed method. As we can see that our proposed method performs better and

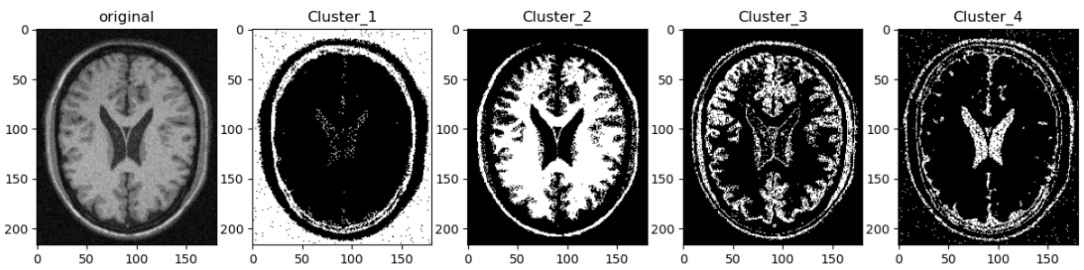



Figure 4.2: Original to Cluster 4 shows the qualitative segmentation results of the Original image, segmented Background image, segmented CSF image, segmented GM image, segmented WM image (from left to right) by the proposed method, on slice 92 of T1-Weighted MR image volume having 9% noise, 40% inhomogeneity.

is more stable with increasing noise and inhomogeneity.

We present the comparative analysis on all of the above four volumes in figure 4.3 of Similarity Index ($\rho$), in figure 4.4 of Partition Coefficient ($V_{pc}$) and in figure 4.5 of Partition Entropy ($V_{pe}$) from which we will be focusing on our best results for further comparison with previous methods over an image volume having 51 (Slice 50 - Slice 100) different T1-Weighted brain MR images.

Table 4.1: Comparative study of average value of Cluster Validity Function (SI ($\rho$), $V_{pc}$, $V_{pe}$) on 51 T1-weighted MRI brain images each in an image volume using different algorithms.

| **Image Volume(Noise%-IIH%)** | **Segmented Method** | **SI(%)** | $V_{pc}$ | $V_{pe}$ |
|---|---|---|---|---|
| 7 – 20 | K-means | 75.578 | ... | ... |
| | FCM | 75.653 | 0.823 | 0.343 |
| | FGFCM | 75.38 | 0.613 | 0.724 |
| | sFCM | 77.723 | 0.912 | 0.153 |
| | ASIFC | 77.072 | 0.866 | 0.294 |
| | **Proposed Method** | **76.91** | **0.824** | **0.303** |
| 7 – 40 | K-means | 74.856 | ... | ... |
| | FCM | 75.656 | 0.823 | 0.343 |
| | FGFCM | 74.782 | 0.592 | 0.762 |
| | sFCM | 76.943 | 0.910 | 0.157 |
| | ASIFC | 76.98 | 0.844 | 0.309 |
| | **Proposed Method** | **76.80** | **0.824** | **0.303** |
| 9 – 20 | K-means | 71.661 | ... | ... |
| | FCM | 71.612 | 0.803 | 0.378 |
| | FGFCM | 71.564 | 0.600 | 0.748 |
| | sFCM | 75.023 | 0.897 | 0.180 |
| | ASIFC | 76.428 | 0.845 | 0.299 |
| | **Proposed Method** | **74.02** | **0.805** | **0.298** |
| 9 – 40 | K-means | 70.431 | ... | ... |
| | FCM | 71.176 | 0.803 | 0.378 |
| | FGFCM | 71.217 | 0.584 | 0.777 |
| | sFCM | 74.351 | 0.897 | 0.180 |
| | ASIFC | 75.580 | 0.843 | 0.290 |
| | **Proposed Method** | **73.40** | **0.805** | **0.298** |

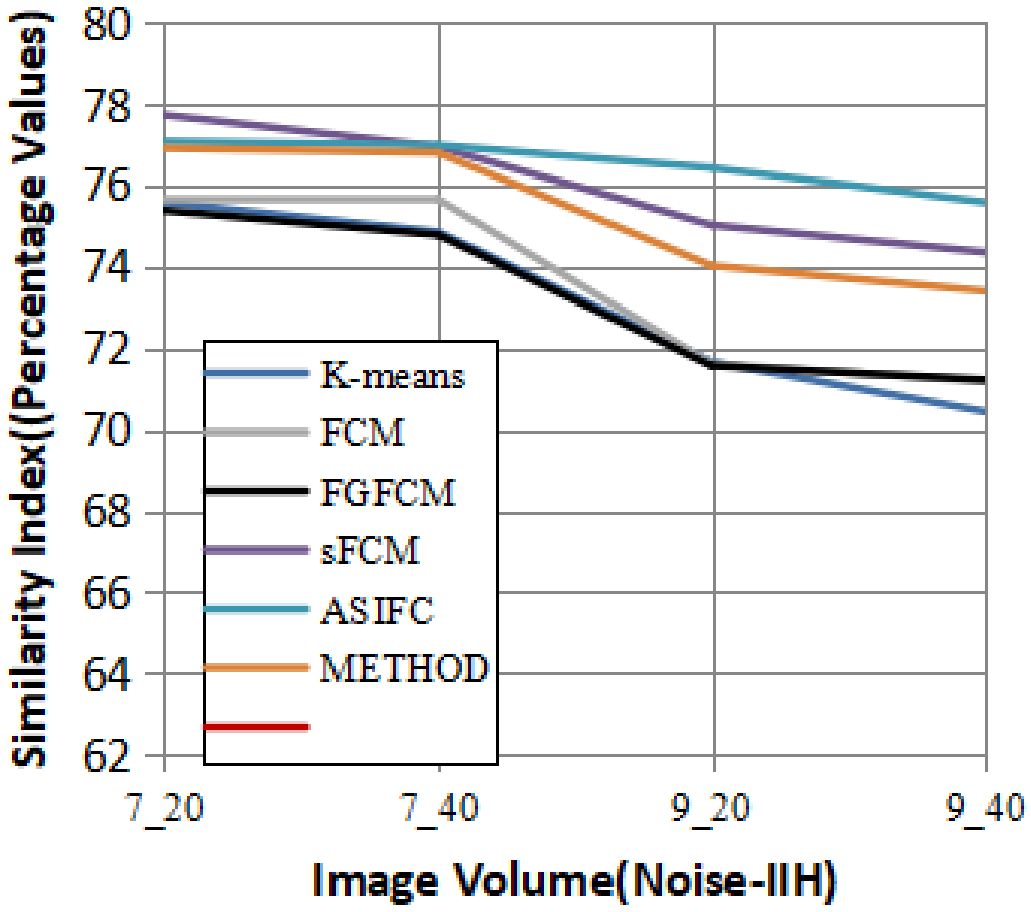



Figure 4.3: Similarity Index ($\rho$) of proposed and other methods

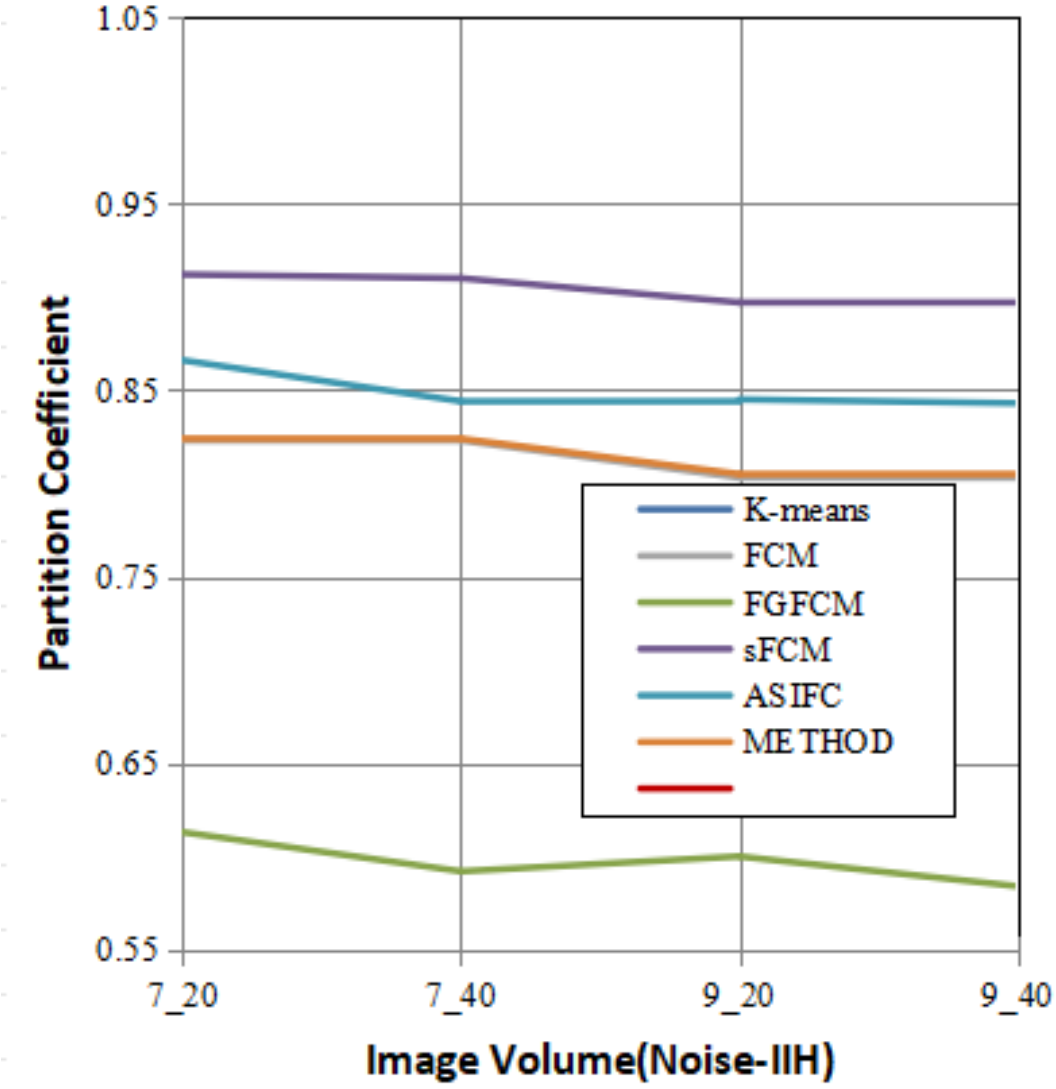



Figure 4.4: Partition Coefficient ($V_{pc}$) of proposed and other methods

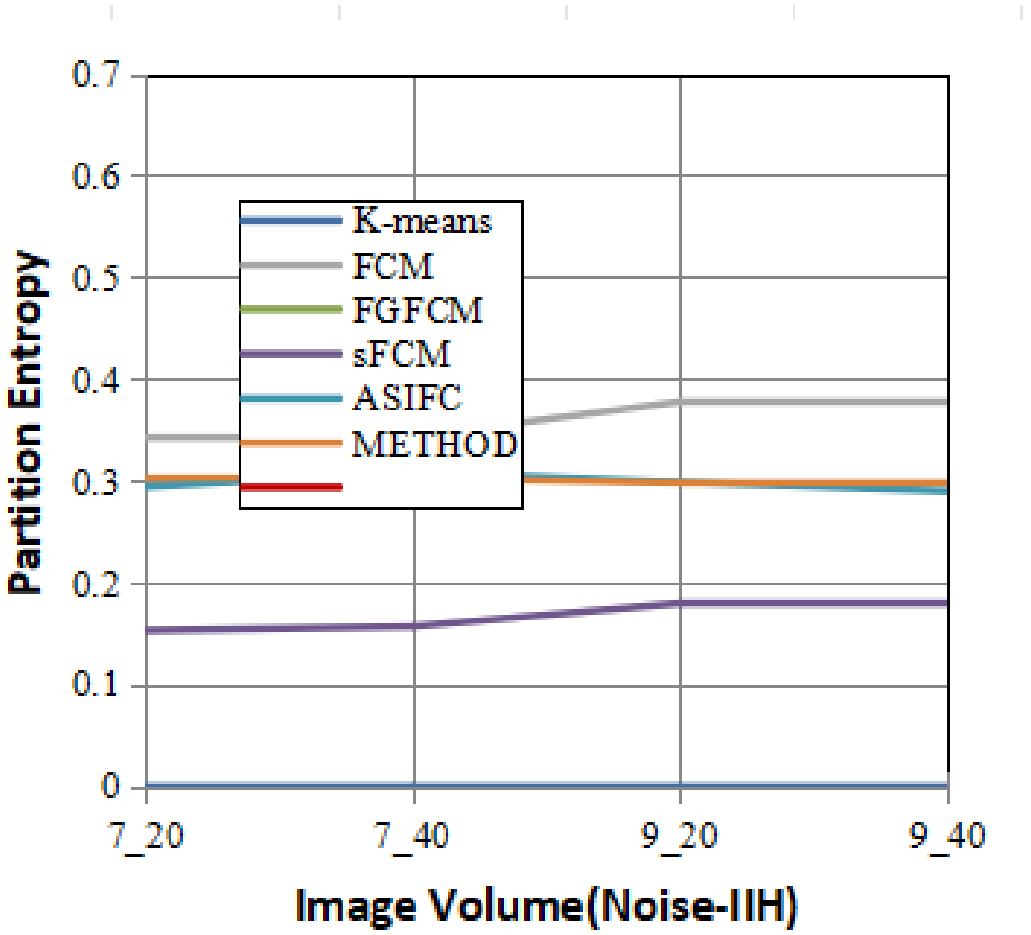



Figure 4.5: Partition Entropy ($V_{pe}$) of proposed and other methods

In the table 4.2 Shows the average values of Segmentation Accuracy (SA) of six different algorithms: The k-means, FCM, FGFCM, sFCM, ASIFC and the proposed method. As we can see that our proposed method performs better and is more stable with increasing noise and inhomogeneity.

Table 4.2: Comparative study of average value of Segmentation Accuracy (SA) on 51 T1-weighted MRI brain images each in an image volume using different algorithms.

| **Segmentation Accuracy(SA)** | | | | | | | |
|---|---|---|---|---|---|---|---|
| **Volumes(Noise%- IIH%)** | **Regions** | **K-means** | **FCM** | **FGFCM** | **sFCM** | **ASIFC** | **Proposed Method** |
| 7 – 20 | CSF | 0.847 | 0.858 | 0.856 | 0.889 | 0.891 | 0.870 |
| | GM | 0.859 | 0.867 | 0.844 | 0.905 | 0.907 | 0.861 |
| | WM | 0.923 | 0.913 | 0.932 | 0.935 | 0.939 | 0.910 |
| 7 – 40 | CSF | 0.845 | 0.858 | 0.853 | 0.888 | 0.890 | 0.870 |
| | GM | 0.859 | 0.860 | 0.836 | 0.896 | 0.899 | 0.864 |
| | WM | 0.885 | 0.890 | 0.912 | 0.909 | 0.913 | 0.887 |
| 9 – 20 | CSF | 0.764 | 0.785 | 0.779 | 0.831 | 0.856 | 0.820 |
| | GM | 0.808 | 0.816 | 0.783 | 0.872 | 0.885 | 0.836 |
| | WM | 0.866 | 0.852 | 0.894 | 0.890 | 0.926 | 0.856 |
| 9 – 40 | CSF | 0.752 | 0.785 | 0.777 | 0.832 | 0.852 | 0.810 |
| | GM | 0.801 | 0.808 | 0.782 | 0.863 | 0.866 | 0.834 |
| | WM | 0.817 | 0.838 | 0.878 | 0.869 | 0.891 | 0.823 |

We present the comparative analysis on all of the above four volumes in figure 4.6 of Segmentation Accuracy (CSF), in figure 4.7 of Segmentation Accuracy (GM) and in figure 4.8 of Segmentation Accuracy (WM) from which we will be focusing on our best results for further comparison with previous methods over an image volume having 51 (Slice 50 - Slice 100) different T1-Weighted brain MR images.

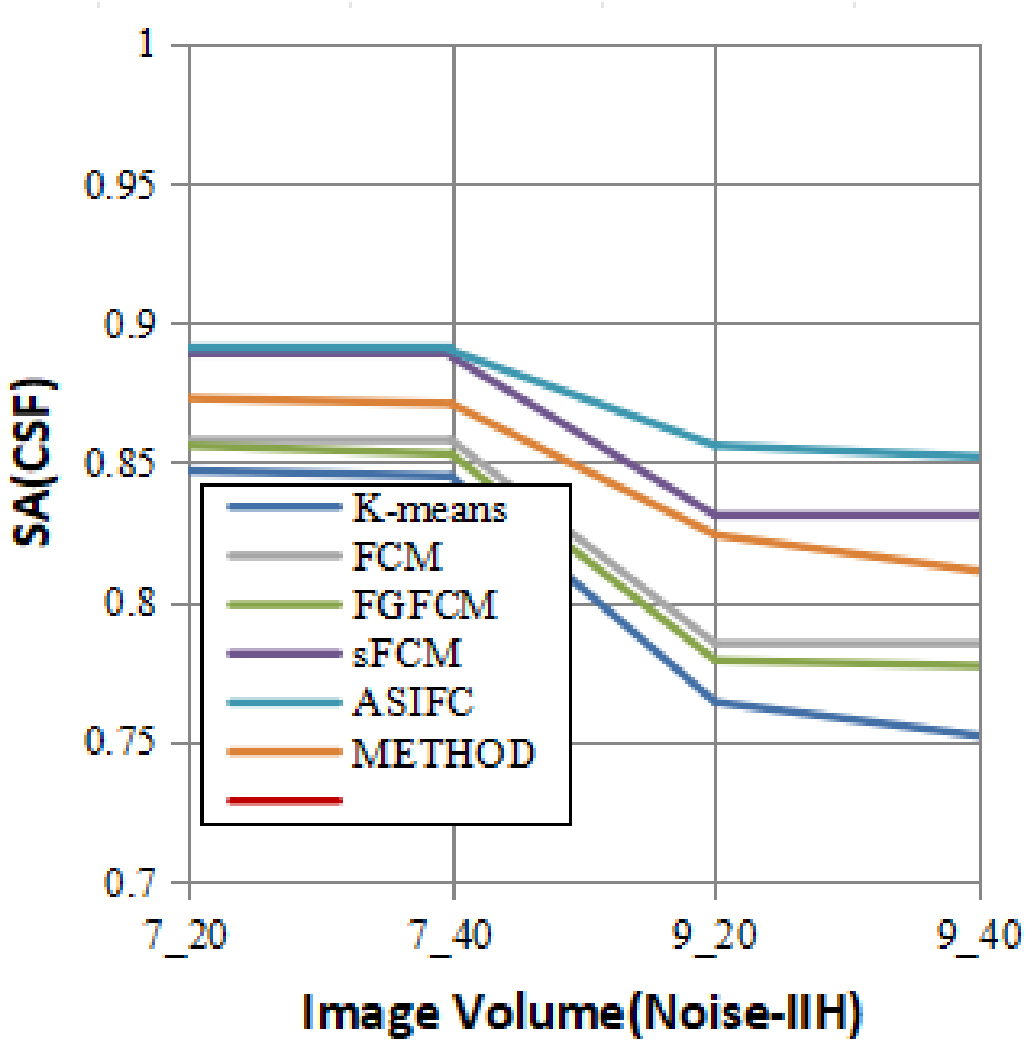



Figure 4.6: Segmentation Accuracy (CSF) of proposed and other methods

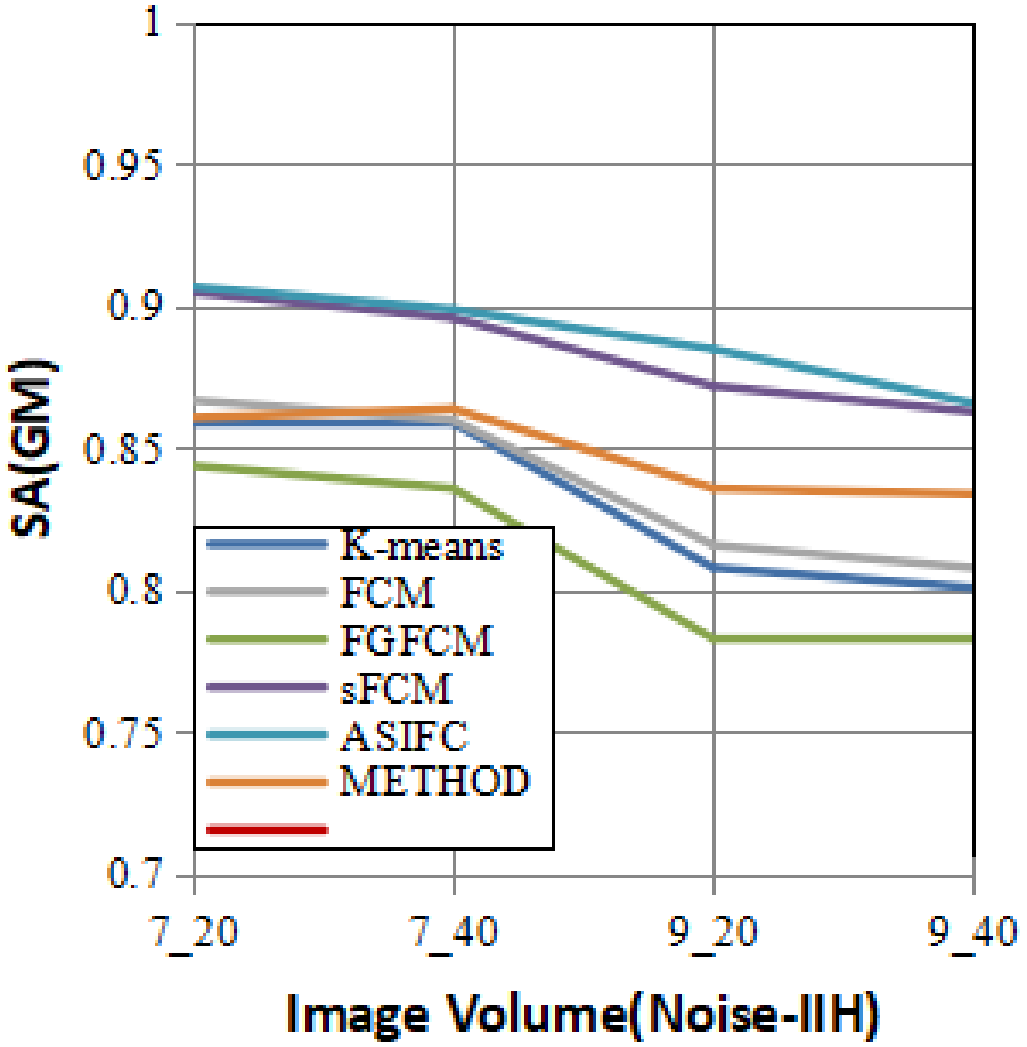



Figure 4.7: Segmentation Accuracy (GM) of proposed and other methods

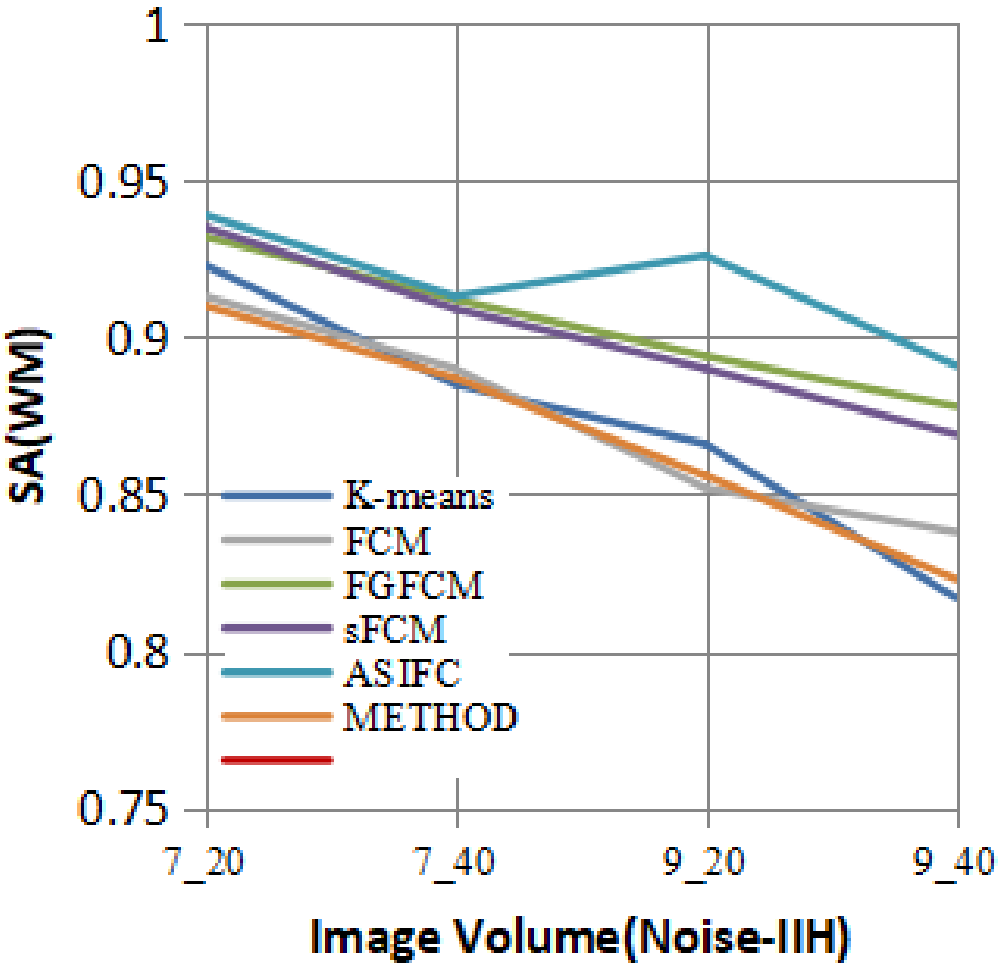



Figure 4.8: Segmentation Accuracy (WM) of proposed and other methods

In the table 4.3 Shows the average values of Tissue Segmentation Accuracy (TSA) of six different algorithms: The k-means, FCM, FGFCM, sFCM, ASIFC and the proposed method. As we can see that our proposed method performs better and is more stable with increasing noise and inhomogeneity.

Table 4.3: Comparative study of average value of Tissue Segmentation Accuracy (TSA) on 51 T1-weighted MRI brain images each in an image volume using different algorithms.

| **Tissue Segmentation Accuracy(TSA)** | | | | | | | |
|---|---|---|---|---|---|---|---|
| **Volumes(Noise%- IIH%)** | **Regions** | **K-means** | **FCM** | **FGFCM** | **sFCM** | **ASIFC** | **Proposed Method** |
| 7 – 20 | CSF | 0.577 | 0.574 | 0.575 | 0.600 | 0.605 | 0.573 |
| | GM | 0.774 | 0.776 | 0.769 | 0.802 | 0.793 | 0.778 |
| | WM | 0.804 | 0.804 | 0.800 | 0.830 | 0.839 | 0.824 |
| 7 – 40 | CSF | 0.566 | 0.570 | 0.571 | 0.598 | 0.599 | 0.561 |
| | GM | 0.766 | 0.765 | 0.759 | 0.789 | 0.788 | 0.754 |
| | WM | 0.799 | 0.796 | 0.793 | 0.820 | 0.827 | 0.812 |
| 9 – 20 | CSF | 0.516 | 0.515 | 0.520 | 0.563 | 0.579 | 0.550 |
| | GM | 0.734 | 0.733 | 0.727 | 0.775 | 0.785 | 0.731 |
| | WM | 0.769 | 0.764 | 0.764 | 0.802 | 0.823 | 0.795 |
| 9 – 40 | CSF | 0.494 | 0.512 | 0.518 | 0.560 | 0.576 | 0.533 |
| | GM | 0.723 | 0.725 | 0.720 | 0.763 | 0.776 | 0.722 |
| | WM | 0.762 | 0.760 | 0.760 | 0.794 | 0.815 | 0.778 |

We present the comparative analysis on all of the above four volumes in figure 4.9 of Tissue Segmentation Accuracy (CSF), in figure 4.10 of Tissue Segmentation Accuracy (GM) and in figure 4.11 of Tissue Segmentation Accuracy (WM) from which we will be focusing on our best results for further comparison with previous methods over an image volume having 51 (Slice 50 - Slice 100) different T1-Weighted brain MR images.

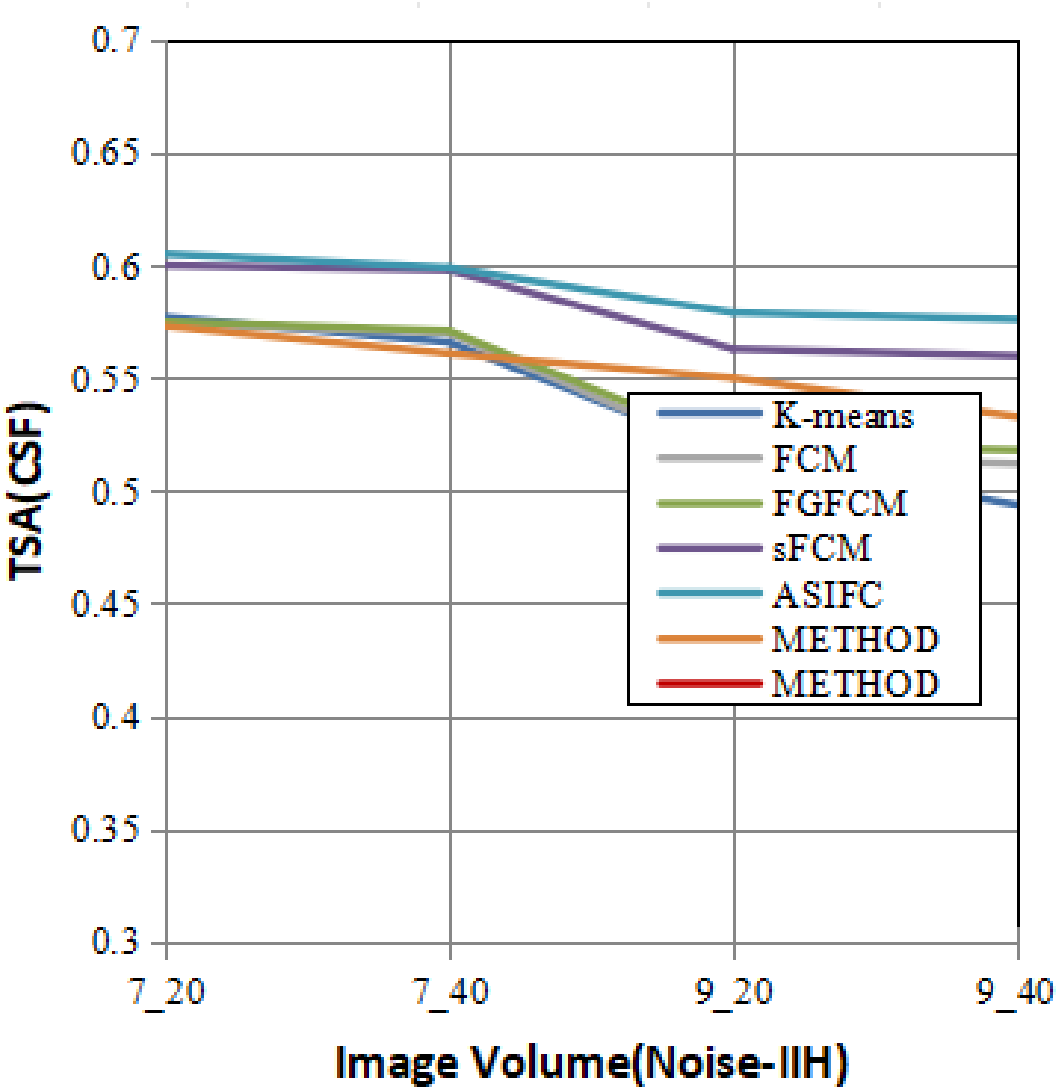



Figure 4.9: Tissue Segmentation Accuracy (CSF) of proposed and other methods

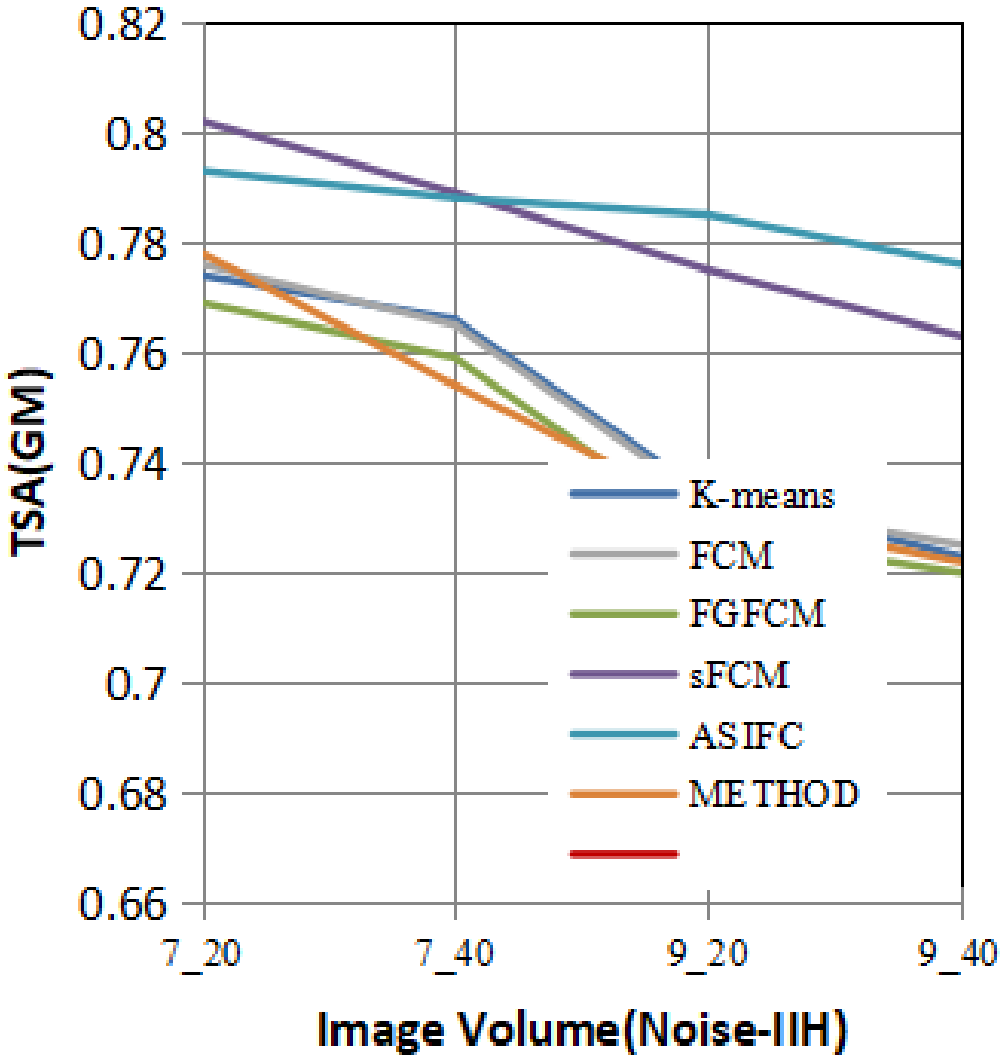



Figure 4.10: Tissue Segmentation Accuracy (GM) of proposed and other methods

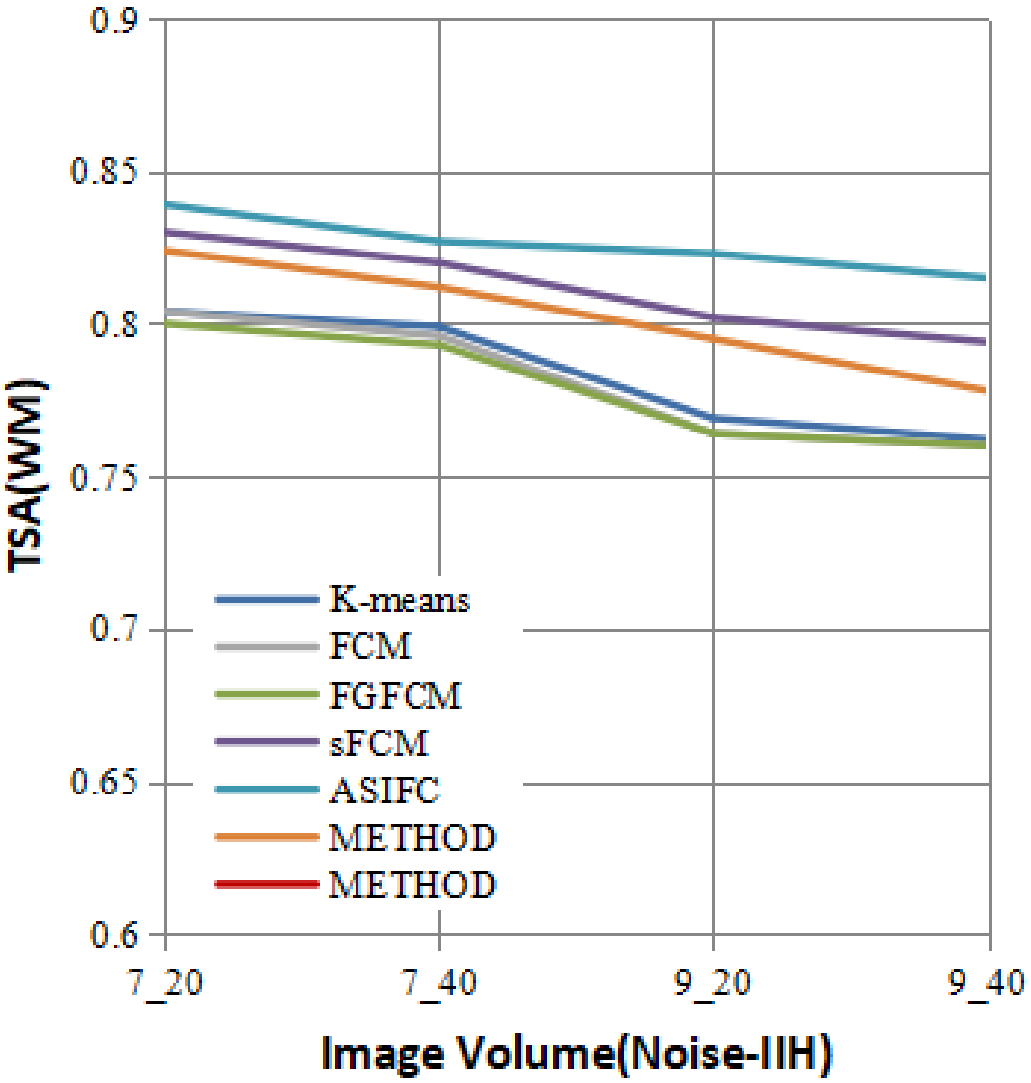



Figure 4.11: Tissue Segmentation Accuracy (WM) of proposed and other methods

CHAPTER 5

# Conclusion

In summary, we have presented a entropy based Fuzzy Clustering Algorithm to segment noisy 2D brain MR image volumes. In particular, the agenda was to improve the robustness to the noise and intensity inhomogeneity involving Shannon entropy. The proposed method in this thesis work, has been examined extensively both in qualitative and quantitative manner. It also has been compared with the k-means, FCM, FGFCM, sFCM and ASIFC algorithm. From the experimental results, we conclude that with proper parameters of neighbourhood and fuzziness the results are definitely better. Also, the proposed method is tolerant to noise and intensity inhomogeneity and thererby it can produce superior results irrespective of the before mentioned hurdles.

# Bibliography


[1] G. Linda, *Shapiro george c. stockman. computer vision*, 2001.

[2] D. Kaur and Y. Kaur, "Various image segmentation techniques: A review," *International Journal of Computer Science and Mobile Computing*, vol. 3, no. 5, pp. 809–814, 2014.

[3] J. S. Duncan and N. Ayache, "Medical image analysis: Progress over two decades and the challenges ahead," *IEEE transactions on pattern analysis and machine intelligence*, vol. 22, no. 1, pp. 85–106, 2000.

[4] Y. Yang, "Image segmentation based on fuzzy clustering with neighborhood information.," *Optica Applicata*, vol. 39, no. 1, 2009.

[5] J. Heil, V. Häring, B. Marschner, and B. Stumpe, "Advantages of fuzzy k-means over k-means clustering in the classification of diffuse reflectance soil spectra: A case study with west african soils," *Geoderma*, vol. 337, pp. 11–21, 2019.

[6] U. Vovk, F. Pernus, and B. Likar, "A review of methods for correction of intensity inhomogeneity in mri," *IEEE transactions on medical imaging*, vol. 26, no. 3, pp. 405–421, 2007.

[7] Z. Hou, "A review on mr image intensity inhomogeneity correction," *International journal of biomedical imaging*, vol. 2006, 2006.

[8] M. A. Balafar, A. R. Ramli, M. I. Saripan, and S. Mashohor, "Review of brain mri image segmentation methods," *Artificial Intelligence Review*, vol. 33, pp. 261–274, 2010.

[9] B. Belaroussi, J. Milles, S. Carme, Y. M. Zhu, and H. Benoit-Cattin, "Intensity non-uniformity correction in mri: Existing methods and their validation," *Medical image analysis*, vol. 10, no. 2, pp. 234–246, 2006.

[10] S. K. Adhikari, J. K. Sing, D. K. Basu, and M. Nasipuri, "Conditional spatial fuzzy c-means clustering algorithm for segmentation of mri images," *Applied soft computing*, vol. 34, pp. 758–769, 2015.

[11] A. Ahmadvand and M. R. Daliri, "Brain mr image segmentation methods and applications," *OMICS J Radiol*, vol. 3, no. 4, e130, 2014.

[12] I. Despotović, B. Goossens, and W. Philips, "Mri segmentation of the human brain: Challenges, methods, and applications," *Computational and mathematical methods in medicine*, vol. 2015, 2015.

[13] D. L. Pham, C. Xu, and J. L. Prince, "Current methods in medical image segmentation," *Annual review of biomedical engineering*, vol. 2, no. 1, pp. 315–337, 2000.

[14] S. D. Olabarriaga and A. W. Smeulders, "Interaction in the segmentation of medical images: A survey," *Medical image analysis*, vol. 5, no. 2, pp. 127–142, 2001.

[15] L. Ma and R. C. Staunton, "A modified fuzzy c-means image segmentation algorithm for use with uneven illumination patterns," *Pattern recognition*, vol. 40, no. 11, pp. 3005–3011, 2007.

[16] F. Tek, A. Dempster, and I. Kale, "Noise sensitivity of watershed segmentation for different connectivity: Experimental study," *Electronics Letters*, vol. 40, no. 21, pp. 1332–1333, 2004.

[17] S. Pereira, A. Pinto, V. Alves, and C. A. Silva, "Brain tumor segmentation using convolutional neural networks in mri images," *IEEE transactions on medical imaging*, vol. 35, no. 5, pp. 1240–1251, 2016.

[18] P. Moeskops, M. A. Viergever, A. M. Mendrik, L. S. De Vries, M. J. Benders, and I. Išgum, "Automatic segmentation of mr brain images with a convolutional neural network," *IEEE transactions on medical imaging*, vol. 35, no. 5, pp. 1252–1261, 2016.

[19] J. Yao, M. Dash, S. Tan, and H. Liu, "Entropy-based fuzzy clustering and fuzzy modeling," *Fuzzy sets and Systems*, vol. 113, no. 3, pp. 381–388, 2000.

[20] M. Zarinbal, M. F. Zarandi, and I. Turksen, "Relative entropy fuzzy c-means clustering," *Information sciences*, vol. 260, pp. 74–97, 2014.

[21] S. Askari, N. Montazerin, M. F. Zarandi, and E. Hakimi, "Generalized entropy based possibilistic fuzzy c-means for clustering noisy data and its convergence proof," *Neurocomputing*, vol. 219, pp. 186–202, 2017.

[22] S. Kannan, S. Ramathilagam, and P. Chung, "Effective fuzzy c-means clustering algorithms for data clustering problems," *Expert Systems with Applications*, vol. 39, no. 7, pp. 6292–6300, 2012.

[23] R. R. Gharieb, G. Gendy, and A. Abdelfattah, "C-means clustering fuzzified by two membership relative entropy functions approach incorporating local data information for noisy image segmentation," *Signal, Image and Video Processing*, vol. 11, pp. 541–548, 2017.

[24] D. Selvathi and R. Dhivya, "Segmentation of tissues in mr images using modified spatial fuzzy c means algorithm," in *2013 International Conference on Signal Processing, Image Processing & Pattern Recognition*, IEEE, 2013, pp. 136–140.

[25] X.-Y. Wang and J. Bu, "A fast and robust image segmentation using fcm with spatial information," *Digital Signal Processing*, vol. 20, no. 4, pp. 1173–1182, 2010.

[26] J. Noordam, W. Van Den Broek, and L. Buydens, "Multivariate image segmentation with cluster size insensitive fuzzy c-means," *Chemometrics and intelligent laboratory systems*, vol. 64, no. 1, pp. 65–78, 2002.

[27] C. Qiu, J. Xiao, L. Yu, L. Han, and M. N. Iqbal, "A modified interval type-2 fuzzy c-means algorithm with application in mr image segmentation," *Pattern Recognition Letters*, vol. 34, no. 12, pp. 1329–1338, 2013.

[28] I. Levner and H. Zhang, "Classification-driven watershed segmentation," *IEEE Transactions on Image Processing*, vol. 16, no. 5, pp. 1437–1445, 2007.

[29] V. Pandey and V. Gupta, "Mri image segmentation using shannon and non shannon entropy measures," *International Journal of Application or Innovation in Engineering & Management*, vol. 3, no. 7, pp. 41–46, 2014.

[30] C. E. Shannon, "A mathematical theory of communication," *The Bell system technical journal*, vol. 27, no. 3, pp. 379–423, 1948.

[31] M. S. Atkins and B. T. Mackiewich, "Fully automatic segmentation of the brain in mri," *IEEE transactions on medical imaging*, vol. 17, no. 1, pp. 98–107, 1998.

[32] S. Sadek and S. Abdel-Khalek, "Generalized $\alpha$-entropy based medical image segmentation," *Journal of Software Engineering and Applications*, vol. 2014, 2013.

[33] C. Lang and H. Jia, "Kapur's entropy for color image segmentation based on a hybrid whale optimization algorithm," *Entropy*, vol. 21, no. 3, p. 318, 2019.

[34] H. Sen and A. Agarwal, "A comparative analysis of entropy based segmentation with otsu method for gray and color images," in *2017 international conference of electronics, communication and aerospace technology (ICECA)*, IEEE, vol. 1, 2017, pp. 113–118.

[35] Z. Wang, Q. Song, Y. C. Soh, and K. Sim, "An adaptive spatial information-theoretic fuzzy clustering algorithm for image segmentation," *Computer Vision and Image Understanding*, vol. 117, no. 10, pp. 1412–1420, 2013.

[36] J. C. Bezdek, "Cluster validity with fuzzy sets," 1973.

[37] J. C. Bezdek, "Mathematical models for systematics and taxonomy," in *Proceedings of the 8th International Conference on Numerical Taxonomy, 1975*, Freeman, 1975.

[38] S. Kahali, S. K. Adhikari, and J. K. Sing, "A two-stage fuzzy multi-objective framework for segmentation of 3d mri brain image data," *Applied Soft Computing*, vol. 60, pp. 312–327, 2017.

[39] BrainWeb, *Brainweb: Simulated brain database (normal brain)*, Accessed: 2024-05-27, 2024.

[40] Internet Brain Segmentation Repository (IBSR), *Internet brain segmentation repository (ibsr)*, Accessed: 2024-05-27, 2024.